An empirical regressive model to improve the metrological performance of mobile spatial coordinate measuring systems

D Maisano* and **L Mastrogiacomo**
Dipartimento di Sistemi di Produzione ed Economia dell'Azienda, Politecnico di Torino, Torino, Italy

The manuscript was received on 15 April 2009 and was accepted after revision for publication on 10 September 2009.

DOI: 10.1243/09544054JEM1604

Abstract: The mobile spatial coordinate measuring system (MScMS) is a system to perform dimensional measurements of large-scale objects. It consists of a wireless measuring probe with ultrasonic (US) transceivers, the position of which is determined using a distributed constellation of analogous transceivers arranged around the measuring area. The principle is to measure the time-of-flight (TOF) of the US signals exchanged between pairs of transceivers and, consequently, to obtain an estimate of their distances. The accuracy of TOF measurements can be attributed to many factors; the most influential are those associated with US signal attenuation.

The purpose of this paper is to build an experimental correction model to reduce the MScMS' error in TOF measurements. First, a two-way block design, which is based on exploratory experiments, is created to show that transmitter–receiver distance and relative orientation between US transceivers have significant effects on TOF measurement error. Next, an empirical regressive model is constructed on the basis of additional detailed experiments. After performing an extensive experimental validation, the model is automatically implemented by MScMS, with an iterative procedure. The most important benefit of such a model is an important reduction in the dispersion and an improved accuracy associated with TOF measurements.

Keywords: large-scale metrology, time-of-flight, ultrasound attenuation, factorial experiment, experimental model

1 INTRODUCTION

The mobile spatial coordinate measuring system (MScMS) is a distributed wireless-sensor-network based system, designed to perform dimensional measurements on large-scale objects [**1**]. The field of large-scale metrology can be defined as the metrology of large machines and structures; specifically, 'the metrology of objects in which the linear dimensions range from tens to hundreds of meters' [**2**]. Typical large objects that can be measured using MScMS are airplane wings, fuselages, longerons of railway vehicles, and boat parts.

**Corresponding author: Production Systems and Business Economics, Politecnico di Torino, Corso Duca degli Abruzzi 24, Torino 10129, Italy.*
email: domenico.maisano@polito.it

MScMS consists of a wireless measuring probe with two ultrasonic (US) transceivers, the position of which is determined using a distributed constellation of other transceivers arranged around the measuring area. These devices, known as Crickets, transmit US signals to each other and measure their time-of-flight (TOF) in order to determine the mutual distances [**3**]. Using this information, MScMS is able to calculate the Cartesian coordinates of the object's surface points touched by the probe.

The introduction of distributed measuring systems, such as MScMS, will probably have important effects on simplifying the current measuring practices within large-scale industrial metrology [**4**]. This tendency is confirmed by other recent distributed measuring systems, such as the Indoor-GPS and the Third Tech Hi-Ball [**5**–**8**]. All these systems have a constellation of distributed devices acting as

reference points for the location of a wireless measuring probe.

Cricket devices are relatively simple and low priced, but not very accurate in estimating the mutual distances. The basic reason is that ultrasound technology can be subject to many error sources; as below [**1**].

1. Speed of sound (s) dependence on environmental conditions – air temperature (T) and relative humidity (RH), which can exhibit both temporal and spatial variations within large working volumes. Since s value makes it possible to turn TOFs into distances, it is required to be often updated, depending on the time and the position. A partial solution to this problem is to use the temperature information evaluated by embedded thermometers at the Cricket receivers and to periodically update s using an experimental relation $s = s(T)$ [**9**].
2. Ultrasound reflections or diffraction, due to the presence of obstacles or external uncontrolled sources of ultrasounds (key jingling, neon blinking, etc.). In order to protect MScMS from these error sources, some statistical tests for online diagnostics are implemented [**10**].
3. Non-punctiform dimension of US transceivers. This makes it difficult to determine the exact point of departure/arrival of a US signal exchanged between a pair of Crickets and consequently to obtain a precise estimate of their distance [**1**].
4. The technique used by Cricket US transceivers for detecting the US signal, known as 'thresholding', is simple to implement but has some drawbacks [**11**, **12**]. More precisely, TOF measurements are corrupted by the US signal attenuation, which may have two major sources:

   (a) transmitter–receiver distance;
   (b) transceivers' relative orientation, as determined by some experimental tests [**13**].

Measurement error is affected by many different factors; however, the most important effects are those related to the sources of US signal attenuation. This is directly caused by the thresholding detection method of ultrasound [**13**]. Other more refined ranging methods are based on phase-detection with fixed-frequency signals and with frequency-modulated signals. The implementation of these techniques, however, would require rather complex modifications to the current Cricket hardware and firmware, such as the introduction of a digital signal processor to process the phase measurements [**11**, **14–18**].

The goal of this paper is to build a two-factor experimental model to improve the accuracy in the MScMSs' TOF measurements, without any modification to the current Cricket hardware. A simpler model was proposed by Moore *et al.* and implemented in a previous version of Cricket firmware [**21**]. However, this model is not very effective in reducing the TOF measurement error derived from the attenuation, because it takes account of the contribution related to the transceivers' distance, but not that related to the transceivers' relative orientation.

The new proposed model can be successfully used at two different stages.

1. In the system set-up, so as to improve the location of the constellation of devices (an operation that has necessarily to be performed before measurements) [**20**].
2. During measurements, so as to improve the accuracy in the location of the wireless probe, which is used to determine the spatial coordinates of the desired points from the measured object surface.

The experimental construction of the model is performed following an analytical protocol, in which the US signal TOF is identified as the key factor (dependent variable) to be examined. Next, two independent variables affecting TOF (transceivers' distance and relative orientation) are varied in order to create a two-way block design with repetition. Air T and RH are fixed and the presentation order is completely randomized to minimize order-of-testing effects. After showing that the two independent variables have a significant effect on the TOF measurement error, additional experiments are performed and a model is constructed by performing a linear regression based on the experimental results. Finally, the empirical model is implemented and validated.

The paper is organized into four sections. Section 2 briefly describes the MScMS structure and features, focusing on the most critical aspects from the metrological performance viewpoint. Section 3 provides a detailed description of the experimental set-up used to determine the input information for constructing the empirical model. Section 4 discusses and analyses the experimental results. In section 5, the model is constructed on the basis of experimental data. An iterative operational procedure for the model online implementation is presented in section 6. The same section presents and discusses the model validation, based on further experimental tests. Finally, the conclusions and future direction of this research are given.

2 SHORT DESCRIPTION AND CRITICAL ASPECTS OF MSCMS

The MScMS prototype consists of three components (Fig. 1).

1. A constellation (network) of Cricket devices arranged around the working area.
2. A measuring probe to communicate with the constellation of devices and obtain the coordinates (x, y, z) of the touched points. More precisely, the measuring probe is a mobile system equipped with a tip to touch the points of the measured objects and a trigger, which is pulled to calculate and store the current coordinates of the probe tip. The constellation Crickets act as reference points for locating the measuring probe [**20**, **21**].
3. A computing system to receive and process data sent by the measuring probe in order to evaluate object geometrical features.

Cricket devices are developed by the Massachusetts Institute of Technology and produced by Crossbow [**3**, **22**]. Being quite small, light, and potentially cheap, they are compatible with a variety of network configurations [**12**, **23**]. All Crickets have radiofrequency (RF) and US transceivers (Fig. 2). They repeatedly communicate and calculate their mutual distances by measuring the TOF of the US signals exchanged [**24**]. TOF is multiplied by the s value to obtain the distance between the two sensors. Thanks to the RF communication, Crickets rapidly share the information about their mutual distances. Crickets, being equipped with embedded processor and memory, can be programmed by the user and customized depending on the communication logic to implement. This flexibility, as well as the relative low cost, is the main reason for their use in MScMS prototype design.

The measuring probe contains two Cricket devices, which repeatedly determine their distance from the constellation Crickets. A Bluetooth transmitter is connected to one of the probe's Crickets in order to send this distance information to a PC, which is equipped with an ad hoc software.

Before starting measurements, the constellation Crickets are placed around the measuring area, so that the region of interest is completely covered with an overlap of at least three devices [**25**]. Next, constellation Crickets have to be localized because measurements are possible only if their position is known. In order to reduce manual operations, a method for a semi-automatic localization has been implemented [**1**, **19**, **25**, **26**].

Measurements consist of three phases:

(a) the mobile probe is used to touch the desired points from the part surface;
(b) the probe trigger is pulled and data are sent via Bluetooth to the PC;
(c) the Cartesian coordinates (x, y, z) of the points are calculated by the PC. The PC then uses the Cartesian points to generate a geometrical model of the measured object's surface [**1**, **19**].

At the time of writing, the MScMS accuracy in determining the spatial position of the measured points may be improved. The most critical aspects influencing the current system's metrological performance are illustrated in sections 2.1 to 2.4 [**1**].

2.1 Cones of vision

While the RF sensor's communication volume is almost omnidirectional and up to 25 m, US sensors have a communication volume limited by 'cones of vision' with an opening angle of approximately 170° and a range of approximately 6 m (Fig. 3). Signal strength inside the cones of vision may be most affected by two factors: the distance and the angle from the transmitter's surface. Outside the cones, signal strength drops to 1 per cent of the maximum value [**27**, **28**].

2.2 Number of constellation devices

For MScMS, the number of constellation devices is strictly related to the measurement volume and their communication range. Some tests show that a coverage of an indoor working volume is achievable with a network density of at least 0.6 devices/m^2, considering a plant layout [**1**]. It should be noticed that the number of constellation devices 'seen' by the

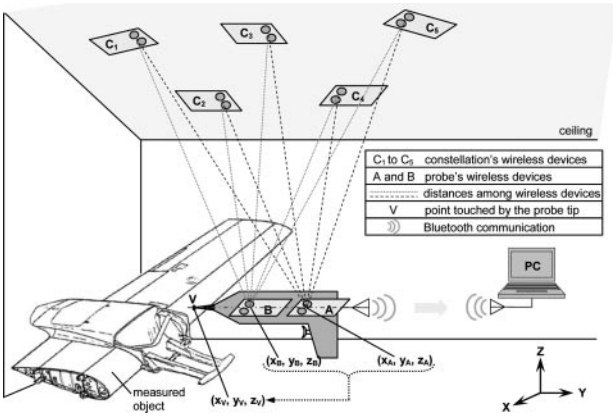

Fig. 1 MScMS representation scheme

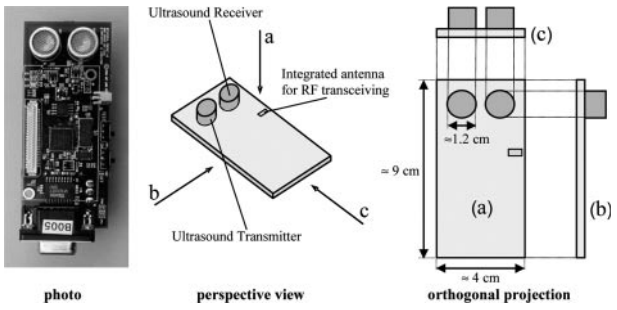

Fig. 2 Cricket device (crossbow technology) [**3**]

sensors has a strong influence on the positioning accuracy. This particular aspect is studied through preliminary tests combined with simulation [**4**].

Specifically, 30 points – with a-priori known positions – are measured (repeating the measurement 150 times per point) while the number of constellation devices for the desired points is deliberately changed from four to 13. Coordinates' position errors (residuals) are determined considering the difference between the 'true' coordinates' position, and the coordinates' position of the points, as calculated by trilateration. The coordinates' position errors related to all the 30 points show a normally distributed pattern, verified by the Anderson–Darling normality test at $p < 0.05$.

The result of the simulation experiment shows that when only four devices are used, the uncertainty in the measured points is very high. This uncertainty decreases to a great extent (for example, by a factor of almost three for the Z axis), when six devices are used for measuring the same point. When the seventh device is added, the improvement in the accuracy reduces, although still significant. By adding the eighth or more transmitters, the improvement is shown to be small and negligible. This behaviour is illustrated in Fig. 4, in which standard deviations (σ_x, σ_y, σ_z) related to the coordinates' positioning errors are plotted based on the number of devices of the constellation.

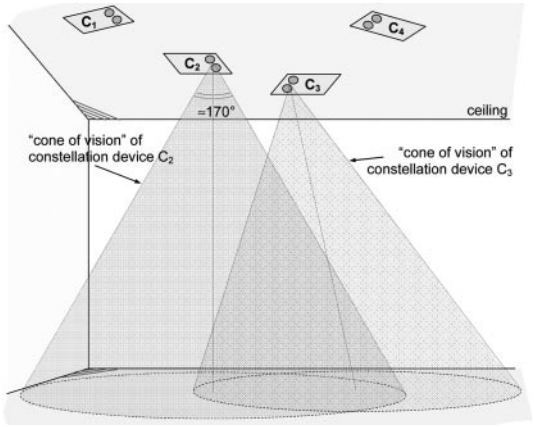

Fig. 3 Representation scheme of the US transmitters 'cones of vision'

Notice that the value of σ_z is basically lower than σ_x and σ_y. This behaviour is due to the geometric configuration of the constellation devices: in general, they are mounted on the ceiling or at the top of the measuring area and, for this reason, they can be considered as approximately placed on a plane (XY) perpendicular to the vertical (Z) axis [**7**].

2.3 Error transmission in the location of Cricket devices

Spatial location of each probe's Cricket is achieved using a trilateration technique [**29**]. The trilateration problem can be solved numerically, by solving a system of n non-linear equations. It is important to remark that input data – (a) constellation device coordinates, and (b) measured distances from the device to locate and the constellation devices – are affected by errors. Specifically, the positioning error of the constellation devices depends on the accuracy of the location procedure implemented. On the other hand, the distance error depends on the measurement error of the corresponding TOF.

Currently, the constellation devices' localization is performed using a reference artefact equipped with several Cricket devices [**1**]. This artefact is placed in different positions within the measuring area. For each of these positions, the TOFs between constellation Crickets and the artefact's Crickets are collected. Next, they are used so as to locate the whole constellation by an ad hoc bundle adjustment algorithm [**19**, **25**]. Thus, the positioning error of the constellation devices is also influenced by the error in TOF measurements.

Summarizing, the two most important error sources in determining the position of a device are (a) the constellation devices positioning error, and (b) the error in the corresponding distance measurements.

2.4 US signal detection technique

Several methods have been developed for detecting US signals [**14**, **15**]. Thresholding is the simplest and the most widely used – both from the hardware and the software points of view [**16**]. In this method, implemented by Crickets, the receiver electric output signal is compared with a threshold level (65 mV for

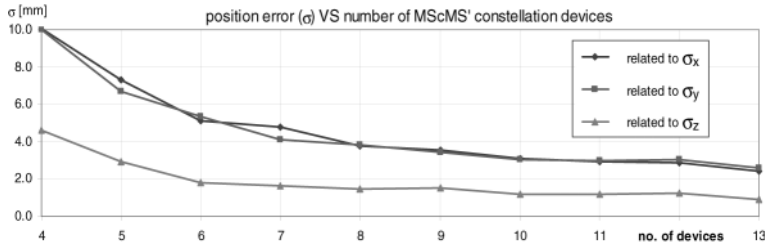

Fig. 4 Influence of the transmitters' number on the position error for MScMS

the Crickets) such that the arrival of the wave is acknowledged when the signal reaches this level (Fig. 5).

This method depends on the amplitude of the pulse received: the larger the signal amplitude, the smaller the time taken by the signal before reaching the threshold. For example, in Fig. 5, when the signal has a full amplitude, the detection threshold is first exceeded by the second peak of the ultrasound waveform. When the waveform is attenuated by a factor of 0.5 (half the amplitude signal), the detection threshold is first exceeded by the third peak of the ultrasound waveform. If the channel attenuation is quite significant, then it may cause the threshold to be exceeded a few periods late instead of just one period late. Consider that at 40 kHz the period is 25 μs, so the error will be in integer multiples of approximately 25 μs. The error in the TOF evaluation results in an error in the distance estimation. The s value is approximately 340 m/s, therefore one ultrasound time period corresponds to a distance of about $25 \bullet 340/1000 = 8.5$ mm. In practice, the threshold can be exceeded by up to four periods late, so the distance overestimation can be up to 3–4 cm!

Typical sources of attenuation are [**3**, **28**]:

(a) distance between transceivers (d);
(b) angle of the transmitter with respect to the transceiver distance (transmitter misalignment angle, $\theta^{(t)}$ in Fig. 6);
(c) angle of one receiver with respect to the transceiver distance (receiver misalignment angle, $\theta^{(r)}$ in Figure 6).

In general, the larger these three factors, the larger the US signal attenuation.

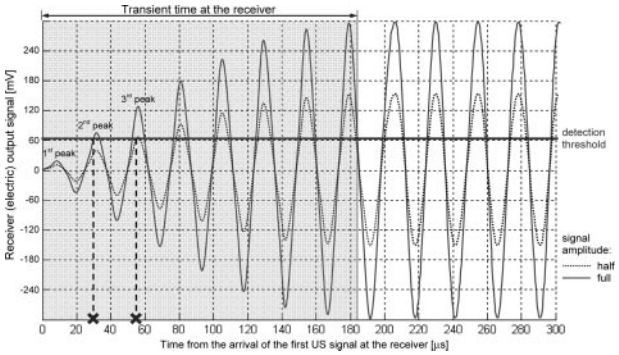

Fig. 5 Graphical representation of thresholding detection. A minimum number of cycles are necessary to bring the receiver to steady state conditions (transient time at the receiver) [**30**]. The error in the distance measurement is dependent upon the received US signal amplitude. The time taken for the received signal to reach the threshold is dependent on its amplitude.

3 DESCRIPTION OF THE EXPERIMENTS

The goal of this work is to obtain an experimental model to correct the TOF-Error derived from the most influential sources of US signal attenuation. Experimental data are collected in the same operational conditions in which the correction model will be used [**31**]; more precisely, constellation devices are assumed to be parallel with respect to the devices to locate. In the current practice, this condition is generally satisfied because constellation devices are arranged on the ceiling, at the top of the measuring area and Crickets to locate are generally mounted on the measuring probe and oriented upwards (Fig. 7). This configuration is a practical solution to obtain a good coverage and to maximize the measuring volume [**28**].

In this configuration, the misalignment angles related to a constellation device (C_i) and the one related to the devices to locate, with respect to their

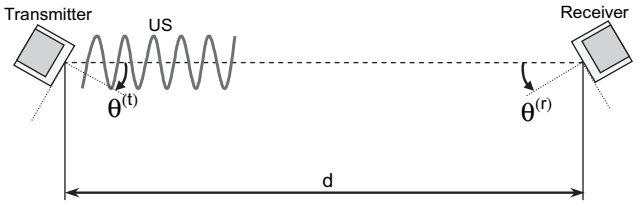

Fig. 6 Illustration of the most important sources of attenuation: transceiver distance (d); transmitter misalignment angle $\theta^{(t)}$, and receiver misalignment angle $\theta^{(r)}$

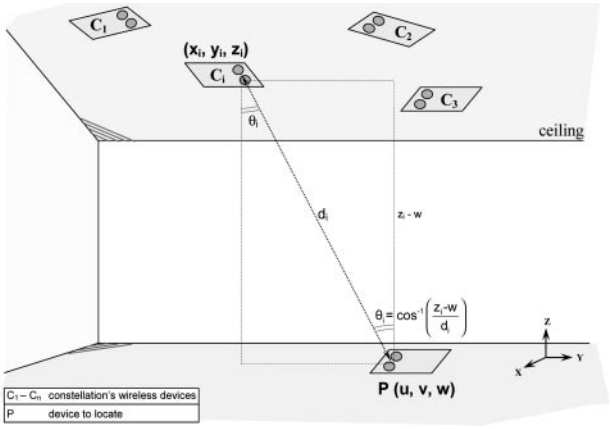

Fig. 7 Typical arrangement of the constellation devices ($C_1 - C_n$). To obtain a good coverage, constellation devices are placed at the top of the measuring area, parallel to the ceiling. With this configuration, Cricket to locate (P) should be oriented upwards. The formula for calculating the misalignment angle (θ_i) is used in the iterative procedure for the TOF-Error correction, reported in section 6.1

distance, is the same (θ_i in Fig. 7). Figure 8 illustrates the experimental set-up:

(a) transmitter and receiver are positioned facing each other;
(b) the distance (d – first factor) between transceivers is known;
(c) transmitter face is parallel with receiver face, but they are not perpendicular with respect to the direction of the distance. A misalignment angle (θ – second factor) is introduced.

As shown in Fig. 8, the reference point for determining the transceivers' distance and misalignment angle corresponds to the centre of the US transceiver cover's face. Distances and angles are measured using a set of calibrated reference bars and a precision goniometer [**32**].

Experiments are organized in two steps.

1. Exploratory experiments. Based on a limited number of observations, this phase is aimed at investigating whether the two factors of interest have significant effects on the TOF measurements. To that purpose, an experimental factorial plan is built measuring TOF and changing the factors at different levels. Table 1 provides a summary of the factor level combinations.
2. Detailed experiments. The factor working domain and the number of observations are increased so as to build an empirical regressive model representing the two factors' effect. Table 2 contains the list of observations considered in this phase.

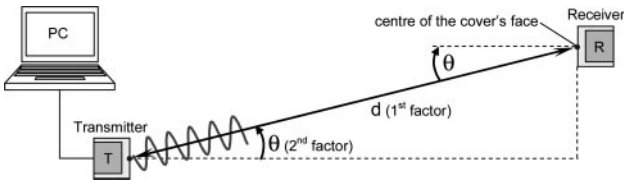

Fig. 8 Experimental set-up

Table 1 List of the experiments carried out in the exploratory phase

	Factors	
	1st – Distance between transceivers (d)	2nd – Transceiver misalignment angle (θ)
Levels	1000	0
	2000	15
	3000	30
		45

– all the possible $3 \times 4 = 12$ different combinations are carried out in random order;
– for each combination, TOF measurements are repeated 50 times;
– all the 12 combinations above are replicated three times; consequently, the total number of combinations is 36. The test sequence is randomized using the random number generator provided by Minitab.

For each of the combinations in Tables 1 and 2, 50 repeated measurements of the TOF are performed.

The response variable considered in the factorial plan is the TOF-Error, which is defined as follows

$$\text{TOF-Error} = (\text{TOF} - \text{Expected-TOF}) \quad (1)$$

being

TOF TOF measured by pair of Crickets;

Expected-TOF $= d/s$ where d is the transceivers known distance and s is the speed of sound in the experimental conditions (with air temperature $T = 21\,^{\circ}\text{C}$ and relative humidity $RH = 27$ per cent, $s \approx 344$ m/s).

TOF-Error is used as an indicator of the error in TOF evaluation.

4 ANALYSIS OF THE EXPERIMENTAL RESULTS

4.1 Results of the exploratory experiments and factorial analysis

Analysing the outputs of the exploratory factorial experiments, notice that TOF-Error dispersion changes depending on the average of the TOF-Error value. This behaviour is illustrated on Fig. 9. For each of the 36 factorial plan combinations, the average TOF-Error and the respective deviations – calculated using the corresponding 50 repeated measurements – are plotted. Notice that the larger the average TOF-Error value, the larger the individual measurement dispersion. The non-homogeneity of the TOF-Error variance is also tested through the Levene statistical test, at $p < 0.05$.

Since the assumption of homogeneity of TOF-Error variances is violated, the Analysis of Variance (ANOVA) cannot be properly applied, in order to verify whether factors have a significant effect on the response (TOF-Error) [**31**]. The usual approach to dealing with non-homogeneous variance is to apply a

Table 2 List of the experiments carried out in the detail phase

	Factors	
	1st – Distance between transceivers (d)	2nd – Transceiver misalignment angle (θ)
Levels	500	0
	1000	15
	1500	30
	2000	45
	2500	60
	3000	
	3500	
	4000	

– all the possible $8 \times 5 = 40$ different combinations are carried out in random order;
– for each combination, TOF measurements are repeated 50 times.

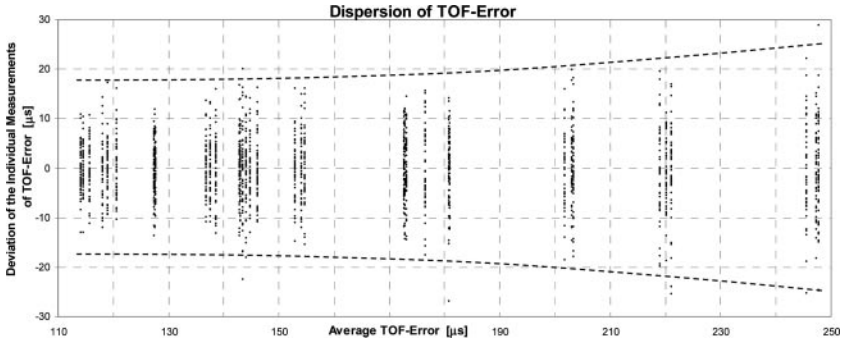

Fig. 9 TOF-Error deviation versus average TOF-Error. For each of the 36 factors combinations, variables are calculated using the corresponding 50 repeated TOF-Error measurements

variance-stabilizing transformation. In this approach, the conclusions of the analysis of variance will apply to the transformed populations. The most common transformation is the exponential $y^* = y^\lambda$, where λ is the parameter of the transformation [**33**, **34**].

The Box–Cox method is used to select λ. The experimenter can analyse the data using $\int \mathrm{y}*$ as the transformed response (hereafter, it will be identified as 'Transformed TOF-Error'). In the authors' specific case, the obtained transformation parameter is $\lambda = 0.17$. Applying Levene's test to the transformed response, the resulting variance no longer violates the test's null hypothesis of homogeneity. To construct a model in terms of the original response, the opposite change of variable $-\ (\mathrm{y}*)^{\frac{1}{\lambda}}$ - is performed.

The main effects plot, representing the single examined factors effect on the TOF-Error, is shown in Fig. 10.

The points in the plot are the means of the response variable at the various levels of each factor (for each level of the examined factor, the mean is calculated averaging all the responses obtained changing the remaining factor). A reference line is drawn at the grand mean of the response data. This kind of plot is useful for comparing magnitudes of main effects. The qualitative result is that d and θ have an important effect.

In order to qualitatively judge the presence of interactions among the two factors, an Interaction Plot is constructed in Fig. 11. Interaction between two factors is present when the response at a factor level depends upon the level(s) of the other factor. Parallel curves in an interactions plot indicate no interaction. The greater the departure of the curves from the parallel state, the higher the degree of interaction [**31**].

Figure 11 shows that the two-way interactions are not very pronounced and that the main effects presented in Fig. 10 are consistent within each factor level.

Results of the factorial plan are examined by ANOVA (Fig. 12).

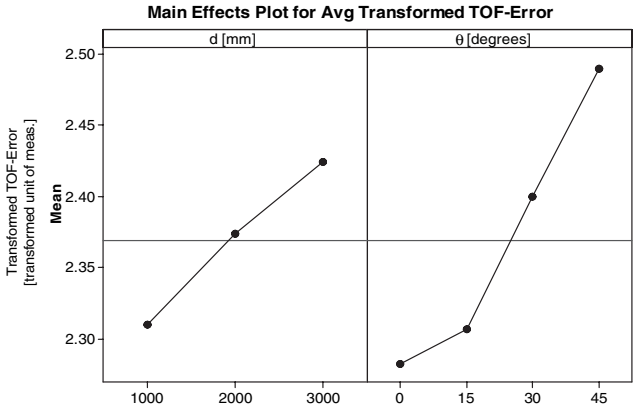

Fig. 10 Main effect plot for means, related to the two examined factors: d (transmitter–receiver distance) and θ (misalignment angle)

In the ANOVA, the variance related to the response is partitioned into contributions owing to the different factors and their interactions. Results of an ANOVA can be considered reliable as long as the following assumptions are met:

(a) the response variable is normally distributed;
(b) data are independent;
(c) variances of populations are equal.

After applying the Box–Cox response transformation, all these assumptions are satisfied. In particular, the assumption of normal distribution is verified by the Anderson–Darling normality test at $p < 0.05$.

Analysing the ANOVA results, all two factors and their two-way interactions are found to be significant based on Fisher's test at $p < 0.05$. With regard to single factors, both d and θ have an important effect. This is consistent with the main effects plot of Fig. 10. With regard to the factor interaction, it is also statistically significant too ($p < 0.05$). Thus, it can be stated that the composition of large misalignment angles (θ) and large distances (d) produces TOF-Errors which are larger than those obtained by adding the effects of the single factors, taken separately.

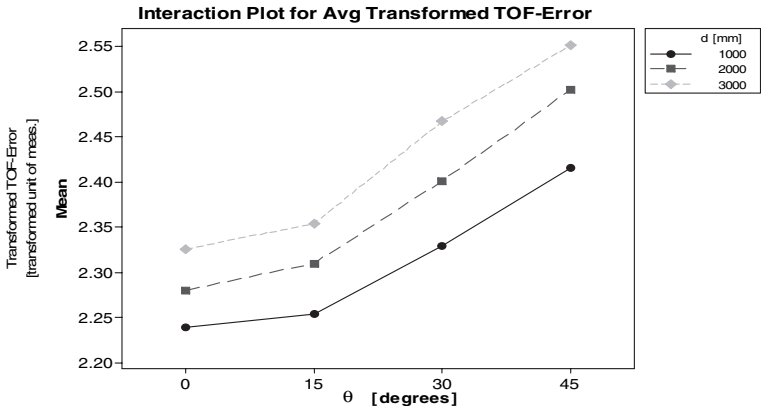

Fig. 11 Interaction plot for transformed TOF-Error, considering the two factors (d and θ)

General Linear Model: Transformed TOF-error versus d and θ

Factor	Type	Levels	Values
d	fixed	3	1000; 2000; 3000
θ	fixed	7	0; 15; 30; 45

Analysis of Variance for Transformed TOF-Error

Source	DF	Seq SS	Adj SS	Adj MS	F	P
d	2	0.078990	0.078990	0.039495	4859.41	0.000
θ	3	0.243035	0.243035	0.081012	9967.54	0.000
d*θ	6	0.003364	0.003364	0.000561	68.97	0.000
Error	24	0.000195	0.000195	0.000008		
Total	35	0.325583				

single factor effect

interactions between factors

Fig. 12 ANOVA applied to the (transformed) response of the factorial plan

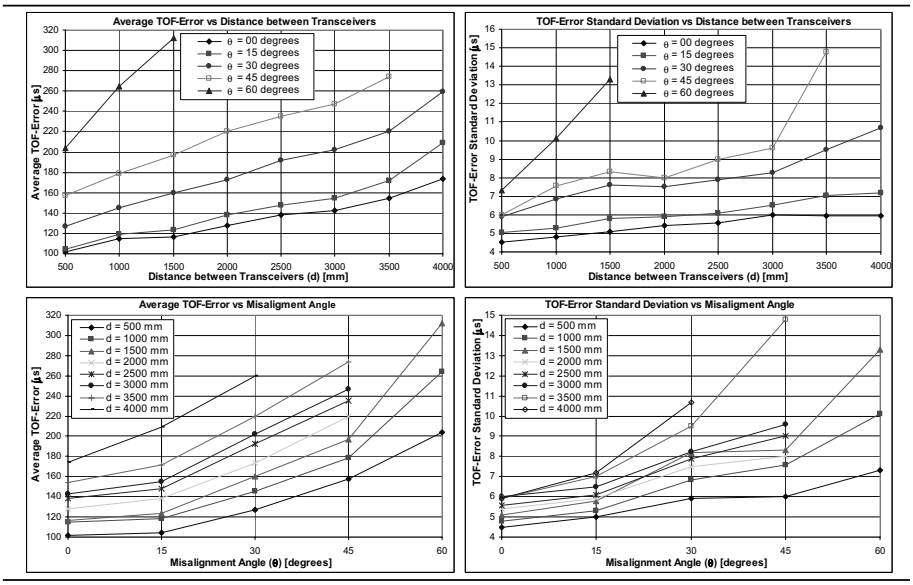

Fig. 13 Average value of the TOF-Error and standard deviation depending on the misalignment angle (θ), for different transmitter–receiver distances (d)

4.2 Results of the detailed experiments

Results of detailed experiments are graphically represented in Fig. 13. They represent the average TOF-Error and the corresponding standard deviation (calculated, for each combination of factors, using the 50 repeated measurements) depending on d and θ. From the two graphs in Fig. 13, it can be noticed that TOF-Error increases with an increase in d and θ. Again, TOF-Error is always positive, because of the TOF overestimation due to the signal attenuation (which is proportional to d and θ). In particular, the relationship between TOF-Error and d appears approximately linear, while the relationship between TOF-Error and θ appears approximately quadratic.

Analysing the graphs in Fig. 13, notice that TOF-Error measurements cannot be performed when the two factors have both large values – i.e. when $\theta = 45°$

Table 3 Communication between transceivers, depending on factors d and q. For some particular combinations of the two factors, transceivers are not able to communicate and – consequently – the experimental table cannot be completely filled. Measurements can be performed precisely only for 37 of 45 (9.5) combinations. When the two factors both have large values – i.e. when $q = 45°$ and $d > 3500$ mm, and when $q = 60°$ and $d > 1500$ mm – measurements are not feasible

		θ [degrees]				
		0	15	30	45	60
d [mm]	500	✓	✓	✓	✓	✓
	1000	✓	✓	✓	✓	✓
	1500	✓	✓	✓	✓	✓
	2000	✓	✓	✓	✓	×
	2500	✓	✓	✓	✓	×
	3000	✓	✓	✓	✓	×
	3500	✓	✓	✓	✓	×
	4000	✓	✓	✓	×	×
	4500	✓	✓	✓	×	×

✓ measurement performed × measurement not feasible

and $d > 3500$ mm, and when $\theta = 60°$ and $d > 1500$ mm (see also Table 3). In fact, in all these conditions, transmitter and receiver are not able to communicate because of the strong signal attenuation (receiver beyond the transmitter's cone of vision).

5 MODEL CONSTRUCTION

In this section an experimental regressive model to link TOF-Error with θ and d is proposed. The total number of observations that are used to construct the model is given by

$$37(\text{combinations}) \cdot 50(\text{repetitions per combination}) = 1850\ \text{TOF(measurements)} \tag{2}$$

Analysing the graph patterns in Fig. 13 and based on the knowledge of the physical phenomenon investigated, a second order polynomial model is chosen (see equation (3)) [**35**]. This model makes it possible to evaluate the factors interaction [**13**]

$$\begin{aligned}&\text{TOF-Error} = C_1 + \\ &C_2 \cdot d + C_3 \cdot \theta + C_4 \cdot d^2 \\ &+ C_5 \cdot \theta^2 + C_6 \cdot d \cdot \theta\end{aligned} \tag{3}$$

With the support of the Minitab Best-Subsets tool, it is found that the terms with coefficients C_3 and C_4 have slightly influential contributions (see results in Fig. 14). Also, this is confirmed by an initial regression, based on the model in equation 3. Consequently, terms with coefficients C_3 and C_4 are removed from the model and a new second order model representing a compromise solution between

Best Subsets Regression:
Average TOF-Error versus d, θ, d², θ² and d·θ

					(C₂)	(C₃)	(C₄)	(C₅)	(C₆)
Vars	R-Sq	R-Sq(adj)	Mallows Cp	S	d	θ	d²	θ²	d·θ
1	72.1	71.2	155.6	28.715					X
1	55.4	54.0	266.8	36.307	X				
2	92.6	92.1	21.4	15.052	X			X	
2	90.1	89.5	37.7	17.359			X	X	
3	95.0	94.5	4.3	11.785	X			X	X
3	94.3	93.7	12.2	13.449		X	X	X	
4	95.7	95.2	7.3	12.566	X	X		X	X
4	95.5	94.8	6.6	12.167	X	X	X	X	
5	95.8	95.0	6.4	11.922	X	X	X	X	X

Fig. 14 Results obtained from Minitab Best-Subsets tool. The above table suggests that the model with the three terms d, θ^2, and $d\theta$ is relatively precise and unbiased because its Mallows' Cp (4.3) is closest to the number of predictors plus the constant (4) [**36**].

best-fitting and reduction of the number of predictors is constructed using equation (4).

$$\begin{aligned}&\text{TOF-Error} = C_1 + C_2 \cdot d \\ &+ C_5 \cdot \theta^2 + C_6 \cdot d \cdot \theta\end{aligned} \tag{4}$$

The model requires the information about the distance and the misalignment angle related to each pair of Cricket devices. Being linear with respect to d and quadratic with respect to θ, the model well represents the graph patterns in Fig. 13. It is important to notice the presence of the last term ($C_6 d\theta$), which accounts for the interaction between the two factors.

Since the variance of the response variable (TOF-Error) is not homogeneous, a simple linear regression is not perfectly suitable. In particular, heteroscedasticity may have the effect of giving too much weight to subset of the data where the error variance is larger, when estimating coefficients. To reduce standard error associated with coefficient estimates, in regression in which homoscedasticity is violated, a common approach is to weight observations by the reciprocal of the estimated point variance [**31**, **34**, **37**]. For each observation, the variance is calculated using the 50 repetitions associated to the corresponding factor combination (numerical values of the σ related to each factor combination are reported in Figure 13). The final regression equation is

$$\begin{aligned}&\text{TOF-Error} = 84.6 + 0.0207d + \\ &0.0314\theta^2 + 0.000336 d\theta\end{aligned} \tag{5}$$

In equation (5), TOF-Error, d and θ are respectively expressed in μs, mm, and degrees.

This model can be useful for correcting the systematic error in TOF measurements. The variation in the response standard deviation being not very large, it was checked that equation (5) is not very dissimilar to the result that would be obtained by a simple (non-weighted) linear regression.

The regression output is quantitatively examined by an ANOVA (Fig. 15). Based on a t test at $p < 0.05$, it can be deduced that all the terms in equation (5) are significant. Examining the residuals, they can be

(Weighted) Regression Analysis: TOF-Error versus d, θ and d·θ

The regression equation is:
TOF-Error = 84.6 + 0.0207·d + 0.0314·θ^2 + 0.000336·d·θ

Predictor	Coef	SE Coef	T	P
Constant	84.6410	0.6040	140.14	0.000
d	0.0206548	0.0002960	69.78	0.000
θ^2	0.0314441	0.0004298	73.15	0.000
d·θ	0.00033568	0.00001144	29.35	0.000

S = 1.65608 R-Sq = 93.9% R-Sq(adj) = 93.8%

Analysis of Variance

Source	DF	SS	MS	F	P
Regression	3	71072	23691	8637.96	0.000
Residual Error	1696	4651	3		
Total	1699	75723			

Source	DF	Seq SS
d	1	18037
θ^2	1	50672
d·θ	1	2362

Fig. 15 Results of the (weighted) regression analysis

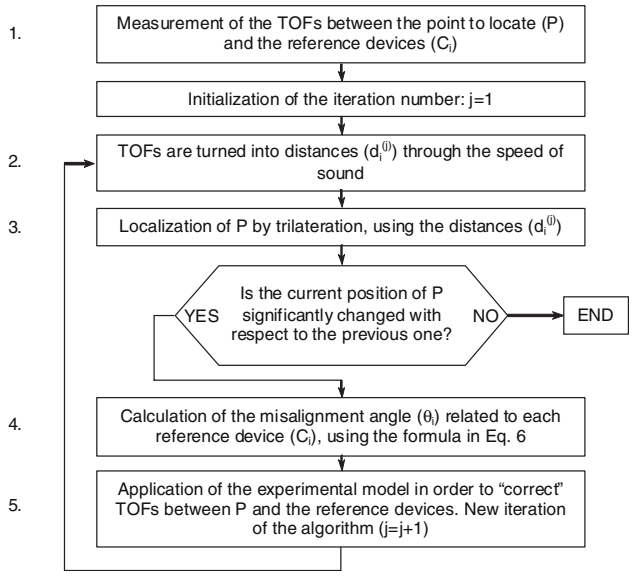

Fig. 16 Flowchart related to the iterative procedure for the model online implementation

considered as randomly distributed by the Anderson-Darling normality test at $p < 0.05$. The model fits the experimental data well.

6 MODEL IMPLEMENTATION AND VALIDATION

6.1 Model online implementation

Considering that reference devices are generally parallel to the device to locate, both during the constellation location and measurements, the experimental model can be implemented online by the following iterative procedure (see flow chart in Fig. 16).

1. TOFs between the device to locate (P) and the reference devices with known position (C_1–C_n) are measured and then the iteration number (j) is initialized to 1.
2. Corresponding distances are calculated as: $d_i^{(j)} = TOF_i^{(j)}s$. Superscript '(*j*)' indicates that the *j*th iteration is considered. Since $TOF_i^{(j)}$ is generally overestimated because of the attenuation, $d_i^{(j)}$ will of course result in being overestimated.
3. Device *P* (with coordinates $u^{(j)}$, $v^{(j)}$, and $w^{(j)}$) is located through a trilateration, using the distances from at least three reference devices with known position (x_i, y_i, z_i).
4. Misalignment angles ($\theta_i^{(j)}$) between device P and each of the reference devices – with which it communicates – are calculated. Because devices have approximately parallel faces, equation (6) can be used (Fig. 7)

$$\theta_i^{(j)} = \cos^{-1}\left(\frac{z_i - w^{(j)}}{d_i}\right) \tag{6}$$

5. Correction of the TOFs associated with each of the reference devices using the following formula:

$$TOF_i^{(j+1)} = TOF_i^{(1)} - \text{TOF-Error}_i^{(j)} \tag{7}$$

where $\text{TOF-Error}_i^{(j)}$ (function of $d_i^{(j)}$ and $\theta_i^{(j)}$) is calculated using the empirical formula in Equation 5.

6. New estimation of the distances ($d_i^{(j+1)}$) between *P* and the devices with known position, and repetition of the procedure (steps 2 to 6, replacing superscripts *j* with $j+1$).

The same procedure can be iterated until changes in the calculated position of *P* are not significant. Conventionally, this condition is reached when the distance between the current position of *P* and the position in the previous iteration is smaller than 1 mm. This algorithm is designed to guarantee convergence to a stable solution. In this sense, this was confirmed to give good results. Typically, no more than three iterations were necessary for the algorithm to converge. Using a standard PC, the total time to complete the procedure was no larger than 0.2 s; therefore, it is fully compatible with the Crickets' TOF measurement sampling period of 0.5 s.

6.2 Model validation

Additional measurements were performed so as to experimentally validate the empirical regressive model in conditions that are representative of the typical working environment. At this stage, a constellation of devices and a set of devices to be measured within the measuring volume were considered. It is important to

remark that the model is based on the assumption that all the Crickets have parallel faces. Unfortunately, this condition cannot be perfectly satisfied in a real measurement context, for two reasons.

1. Devices of the constellation are not perfectly parallel to each other. This condition would slow down and complicate the manual arrangement of constellation devices and compromise the MScMSs' easy start-up [**1**]. It was experienced that, in a typical (quick) arrangement, misalignments of constellation devices with respect to the 'ideal' parallelism condition are included within 3° [**23**].
2. Devices to be measured, which are mounted on the mobile probe, are not necessarily parallel to constellation devices. In fact, during the measurement task it is very difficult to keep the mobile probe always horizontal and facing constellation devices, due to the shape of the measured object. The mobile probe's misalignment with respect to the 'ideal' orientation was seen to be up to 10–15° [**23**].

Thus, to test the efficiency of the proposed model in realistic measurement conditions, small misalignments – of the same amount as before – were deliberately introduced both for constellation devices and devices to be measured. More precisely, measurements were carried out in the following way:

- A limited indoor measuring volume of about 24 m^3 ($4 \times 3 \times 2$) is considered. Eight constellation devices are distributed at the top of the volume, and a planar density of about 0.7 devices/m^2 (Fig. 17). The rough position of each device is randomly decided using a random number generator.

Then, in line with the previous experiments (Fig. 8), the 'reference' position of each device – the Cartesian coordinates of the point coinciding with the centre of the transceiver cover's face – is calculated using a laser-tracker. Because of the transceiver's relatively small dimensions, it is difficult to measure the cylindrical cover touching it directly with the laser-tracker (cat's-eye) retroreflector. Therefore, measurements are performed using a support 'cap' – i.e. an auxiliary component consisting of a hollow cylinder surmounted by a hemisphere. More precisely, the internal hole of the cap fits the US transducer's cover, so that, when the transducer is 'capped', the centre of the cover's face coincides with the centre of the cap hemisphere (Fig. 18(b)). For the Crickets oriented downwards, i.e. those arranged on the ceiling, the cap is fixed to the Cricket board using some plasticine. The cap is made of aluminium and manufactured using a CNC turning lathe with typical uncertainty of approximately a few hundredths of a millimetre.

The measurement procedure consists in:

(a) 'capping' the transducer with the support cap;
(b) measuring several points (i.e. four or more), which are uniformly distributed on the hemisphere surface, using the laser-tracker retroreflector (Fig. 18(a));
(c) determining the coordinates (x, y, z) of the hemisphere centre through a standard optimization algorithm.

A preliminary uncertainty budget is constructed considering the uncertainty related to:

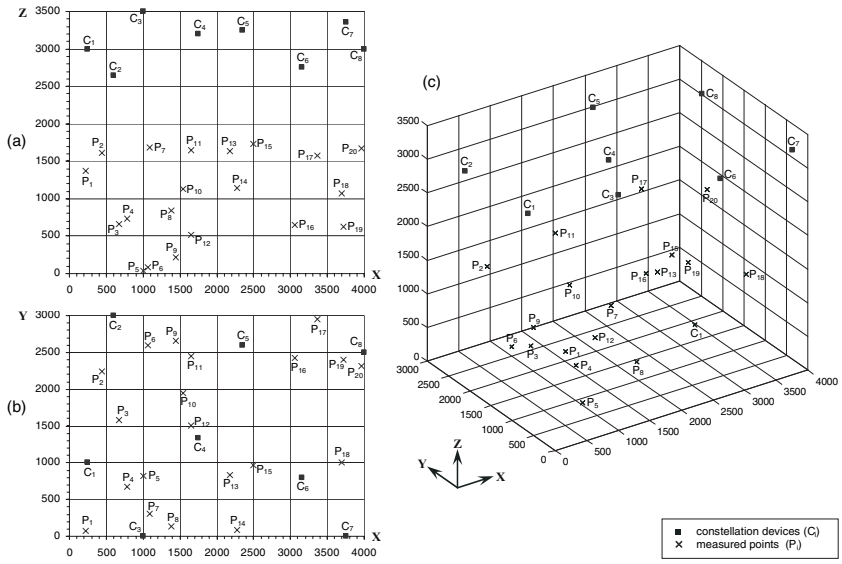

Fig. 17 Representation of the experimental set-up used for the validation experiment. Specifically, (a) *XZ* plane view, (b) *XY* plane view, (c) 3D view. The measuring volume contains eight constellation devices (■) and 20 measured points (×), which are randomly positioned

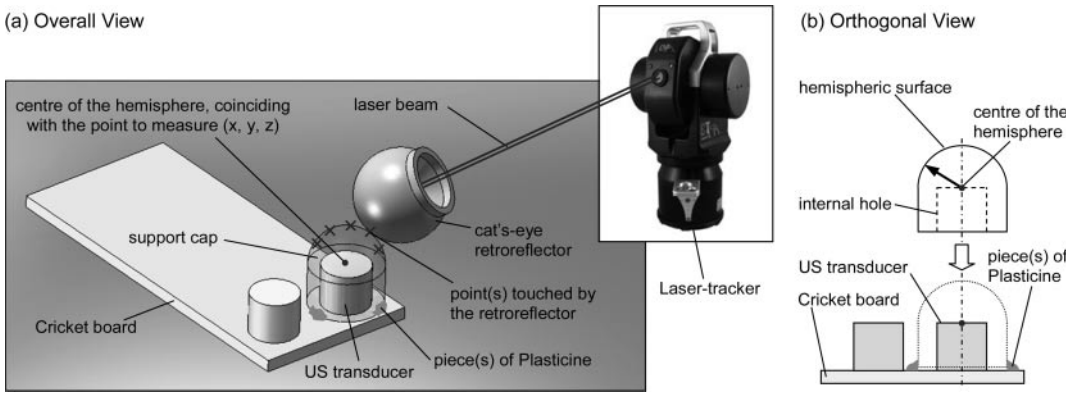

Fig. 18 Representation scheme of the procedure to calculate the coordinates of the point in the middle of the face of the US transducer cover

(a) the dimensional features of the support cup;
(b) the laser-tracker measurement of the points on the cap hemispheric surface;
(c) the algorithm to determine the centre of the hemisphere, using the previous points.

The result is that the error associated to the coordinates of the point to measure is reasonably smaller than one millimetre, which is one to two orders of magnitude more accurate than the Cricket distance measurements [**38**–**40**].

- A Cricket device is placed next to 20 representative points that are positioned within the measuring volume. The approximate position of each point is randomly decided using a random number generator. Next, the 'reference' position is measured by a laser-tracker with the same procedure as before. For each of the 20 points, eight TOFs from the corresponding constellation devices are collected replicating the individual measurements five times. In practice, the device to be located is moved and repositioned before each measurement, with the aim of reproducing the usual measurement conditions. Thus, $20 \times 8 \times 5 = 800$ total TOF measurements (number of measured points × number of constellation devices × replications). These TOFs are turned into corresponding distances applying the iterative procedure seen in section 6.1. Then, distance values are compared with the corresponding reference values – derived using the laser-tracker reference positions – so as to calculate the resultant error. Results obtained by the application of the experimental model are compared (a) with the results obtained by applying a first order one-factor model, which was proposed by Moore *et al.* [**21**] and implemented in a previous version of Cricket firmware (see equation (8)), and (b) with the results obtained with no correction

$$d_i = 49.671 + 0.00096 \times s \times \mathrm{TOF}_i \qquad (8)$$

Table 4 Results of validation experiments with regard to the Cricket distance error. Notice that the two-factor correction model, compared to the one-factor model, makes it possible to reduce the dispersion in the distance evaluation considerably. Moreover, results obtained with no correction are very poor, both in terms of centring ($m_{d\text{-error}} = 70.5$ mm! due to the systematic TOF measurement overestimation) and dispersion ($s_{d\text{-error}}$)

Distance error	Two-factor experimental model	One-factor experimental model	No correction
$\mu_{d\text{-error}}$ [mm]	−0.3	0.6	70.5
$\sigma_{d\text{-error}}$ [mm]	5.6	9.8	15.9

$\mu_{d\text{-error}}$ and $\sigma_{d\text{-error}}$ are calculated considering 800 individual distance evaluations, performed in random order.

Reference distances are obtained using a laser-tracker (see Fig. 18), with a measurement uncertainty one–two orders of magnitude smaller than Crickets'.

In equation (8), d_i, s, and TOF_i are respectively expressed in mm, m/s, and μs.

Using the one-factor model in equation (8), distances (d_i) can be calculated from the corresponding $\mathrm{TOF}_i s$. Unlike the two-factor model, this model only accounts for the attenuation effect due to d, but does not consider the effect of θ.

In summary, the distance error is calculated in the three following situations:

(a) application of the two-factor empirical model;
(b) application of the one-factor model;
(c) no correction.

Next, the average value ($\mu_{d\text{-error}}$) and the standard deviation ($\sigma_{d\text{-error}}$) related to distance error are calculated. Results are reported in Table 4. It is relevant to emphasize that these errors are not overall uncertainties for the system, because they are not achieved

when all the error sources are combined in an uncertainty budget, also including traceable calibration uncertainties of the reference artefacts [**39**, **41**].

Notice that the two-factor correction model, compared to the one-factor model, makes it possible to reduce the dispersion in the distance evaluation considerably. Specifically, reduction is larger than 40 per cent – i.e. $(9.8 - 5.6)/9.8$. The price to pay is that the two-factor model is based on the assumption that constellation devices are parallel with respect to the device to locate (Fig. 7). Also, from Table 4, notice that results obtained with no correction are very poor, both in terms of centring (large $\mu_{d\text{-error}}$, due to the systematic TOF measurement overestimation) and dispersion ($\sigma_{d\text{-error}}$). In this case, the reduction of the dispersion is larger than 60 per cent – i.e. $(15.9 - 5.6/15.9)$.

Depending not on the constellation device density – but only on the TOF measurements between device to locate and constellation devices, these results can be extended to constellations with a different density.

It is important to remark that the two-factor model was obtained under a precise air condition T and RH ($T = 21\,^{\circ}\text{C}$ and $RH = 27$ per cent). In theory, the model should be used in these precise conditions and, for different T and RH values, it is no longer valid. US signal attenuation, which is the main source of TOF estimation errors, and the speed of sound (s) value are both influenced by air T and RH [**34**]. In general, the effect of RH can be neglected, especially for moderate variations (i.e. ΔRH not larger than 30–40 per cent – conditions generally satisfied within shop-floors). Moreover, if T variations are limited (i.e. ΔT contained within 8–10 °C – condition generally satisfied within shop-floors), the effect of T on ultrasound attenuation can be neglected also [**9**, **42**]. Thus, the only effect to be compensated is that of T on s. To that purpose, T is periodically evaluated by embedded thermometers at the Cricket receivers and s is automatically updated using an experimental relation $s = s(T)$ [**1**].

Referring to the validation experiments, the position of the 20 points is calculated by trilateration of the distances from the eight constellation devices. The average position error ($\mu_{\text{position-error}}$), calculated with respect to the laser-tracker reference positions, and the corresponding standard deviations ($\sigma_{\text{position-error}}$) are reported in Table 5. Again, those results obtained applying – in the same conditions – the one-factor model and those obtained with no correction are compared.

Again, results show that the two-factor model makes it possible to improve the position accuracy significantly. Notice that the σ_z values are generally lower than σ_x and σ_y. This behaviour is due to the geometric configuration of the constellation devices, as explained in section 2.2.

7 CONCLUSIONS

This paper proposes an experimental model to reduce the error in the TOF measurement among MScMS' Crickets. Being the most important error sources, the model takes the transceiver distance and the misalignment angle into account. Both these factors are related to the US signal attenuation and, by reason of an empirical factorial analysis, it is shown that the factors and their interaction have significant effects on TOF-Error.

An empirical regressive model is constructed on the basis of experimental data and successively validated through additional experiments. The model is based on the assumption that the Cricket devices in communication have parallel faces. In common practice, this condition is respected approximately because constellation devices are arranged on the ceiling above the measuring area and the face of the device to locate is roughly parallel to them. In the validation, results provided by the correction model are compared with those obtained applying respectively:

(a) a one-factor model;
(b) with no correction.

The most important benefit of the two-factor model is a reduction in the dispersion associated with TOF measurements: specifically, more than

Table 5 Results of validation experiments with regard to the positioning error. The two-factor correction model, compared to the one-factor model, makes it possible to reduce the dispersion in the position error considerably. Besides, results obtained with no correction are very poor, both in terms of centring and dispersion, because of the systematic overestimation of the distances between constellation devices and points to locate

Position error related to the single coordinates	Two-factor experimental model			One-factor experimental model			No correction		
	Δx	Δy	Δz	Δx	Δy	Δz	Δx	Δy	Δz
$\mu_{\text{position-error}}$ [mm]	1.3	3.3	−1.0	−4.0	12.7	0.2	−4.8	23.8	−69.5
$\sigma_{\text{position-error}}$ [mm]	6.4	6.2	2.3	9.5	10.4	2.8	25.9	26.6	2.6

Reference positions of the twenty measured points are obtained using a laser-tracker (see Figure 18), with a measurement uncertainty one-two orders of magnitude smaller than Crickets'

40 per cent with respect to the one-factor model and more than 60 per cent with respect to the case with no correction. The two-factor model can be automatically implemented by Crickets with an iterative procedure, and profitably used both in the measurement and in the constellation location phases. The model is effective provided that air T is around 21 °C, with variations not larger than 8–10 °C; however, this condition is generally satisfied within shop-floors. It is remarkable that, requiring no extra hardware or software equipments, the model makes it possible to enhance the MScMS metrological performance, with no additional effort. Even if, in the future, the MScMS technology could be substantially improved, the proposed methodology can still be relevant to correct other error sources in a homologous way.

Regarding the future, a more refined correction model, which takes account of the fact that during the measurement task the mobile probe's devices are not perfectly parallel to constellation devices, will be studied. In fact, it is very difficult to keep the mobile probe always horizontal and facing the constellation devices, owing to the shape of the measured object. Furthermore, Cricket's accuracy could be improved using more refined ranging methods based on US pulse compression, so as to reduce the transceiver angular sensitivity substantially. This should be obtained with some modifications to the current Cricket hardware and firmware. Another possible solution to the error associated with transmitter misalignment is the use of US transducers which present a smaller directivity, such as cylindrical polyvinylidene fluoride (PVDF) film transducers [**43**, **44**]. Also, other experiments will be carried out in order to study the best way of positioning the MScMS constellation devices, depending on the measured object and the working volume layout [**23**].

REFERENCES

1 **Franceschini, F., Galetto, M., Maisano, D.,** and **Mastrogiacomo, L.** Mobile spatial coordinate measuring system (MScMS) – introduction to the system. *Int. J. Prod. Res.*, 2009, **47**(14), 3867–3889.

2 **Puttock, M. J.** Large-scale metrology. *Ann. CIRP*, 1978, **21**(1), 351–356.

3 MIT Computer Science and Artificial Intelligence Lab, Cricket v2 user manual, 2004, available from *http://cricket.csail.mit.edu/v2man.html*.

4 **Maisano, D., Jamshidi, J., Franceschini, F., Maropoulos, P., Mastrogiacomo, L., Mileham, A.,** and **Owen, G.** Comparison of two distributed large volume measurement systems: MScMS and iGPS. *Proc. IMechE, Part B: J. Engineering Manufacture*, 2009, **223**(B5), 511–521. DOI: 10.1243/09544054JEM1271.

5 ARC Second, Product literature, 2004, available from *URL http://arcsecond.com*.

6 Metris, 2008, available from *e URL http://www.metris.com*.

7 **Maisano, D., Jamshidi, J., Franceschini, F., Maropoulos, P., Mastrogiacomo, L., Mileham, A.,** and **Owen, G.** Indoor GPS: system functionality and initial performance evaluation. *Int. J. Mfg Res.*, 2008, **3**(3), 335–349.

8 **Welch, G., Bishop, G., Vicci, L., Brumback, S.,** and **Keller, K.** High-performance wide-area optical tracking the HiBall tracking system. In *Presence: Teleoperators and Virtual Environ.*, 2001, **10**(1), 1–21.

9 **Bohn, D. A.** Environmental effects on the speed of sound. *J. Audio Engng Soc.*, 1988, **36**(4), 223–231.

10 **Franceschini, F., Galetto, M., Maisano, D.,** and **Mastrogiacomo, L.** On-line diagnostics in the mobile spatial coordinate measuring system. *Precision Engng*, 2009, **22**(7), 698–716.

11 **Piontek, H., Seyffer, M.,** and **Kaiser, J.** Improving the accuracy of ultrasound-based localisation systems. *Personal and Ubiquitous Comput.*, 2007, **11**(6), 439–449.

12 **Priyantha, N. B., Chakraborty, A.,** and **Balakrishnan, H.** The Cricket location-support system. In Proceedings of the Sixth ACM *MOBICOM*, Boston, MA. 2000.

13 **Franceschini, F., Maisano, D., Mastrogiacomo, L.,** and **Pralio, B.** Ultrasound transducers for large-scale metrology: a performance analysis for their use by the MScMS. *IEEE Trans. on Instrumn and Measmt*, 2009, **58**(11), 1–12.

14 **Patwary, N., Ash, J., Kyperountas, S., Hero III, A., Moses, R.,** and **Correal, N.** Locating the nodes – cooperative localization in wireless sensor networks. *IEEE Signal processing Mag.*, 2005, **22**(4), 54–69.

15 **Martin, J. M., Jiménez, A. R., Seco, F., Calderon, L., Pons, J. L.,** and **Ceres, R.** Estimating the 3D-position from time delay data of US-waves: experimental analysis and new processing algorithm. *Sensors and Actuators*, 2002, **101**(3), 311–321.

16 Crossbow Technology, 2009, available from *URL http://www.xbow.com*.

17 **Balakrishnan, H., Baliga, R., Curtis, D., Goraczko, M., Miu, A., Priyantha, N. B., Smith, A., Steele, K., Teller, S.,** and **Wang, K.** Lessons from developing and deploying the Cricket indoor location system, 2003 (Preprint).

18 **Gustafsson, F.** and **Gunnarsson, F.** Positioning using time difference of arrival measurements. In Proceedings of the IEEE International Conference on *Acoustics, speech and signal processing (ICASSP 2003)*, Hong Kong, 2003, vol. 6, pp. 553–556.

19 **Franceschini, F., Galetto, M., Maisano, D.,** and **Mastrogiacomo, L.** A review of localization algorithms for distributed wireless sensor networks in manufacturing. *Int. J. Computer Integrated Mfg*, 2009, **22**(7), 698–716.

20 **Mahajan, A.** and **Figueroa, F.** An automatic self-installation and calibration method for a 3D position sensing system using ultrasonics. *Robotics and Autonomous Syst*, 1999 (28), 281–294.

21 **Moore, D., Leonard, J., Rus, D.,** and **Teller, S. S.** Robust distributed network localization with noisy range

measurements. In *Proceedings of SenSys 2004*, Baltimore, MD, pp. 50–61.

22 **Priyantha, N. B., Balakrishnan, H., Demaine, H. D.,** and **Teller, S.** Mobile-assisted localization in wireless sensor networks. In Proceedings of the 24th Annual Joint Conference of the IEEE Communications Society on *Computer communications (INFOCOM 2005)*, Miami, Florida, 13–17 March 2005, vol. 1, pp. 172–183.

23 **Franceschini, F., Galetto, M., Maisano, D.,** and **Mastrogiacomo, L.** The problem of distributed wireless sensors positioning in the mobile spatial coordinate measuring system (MScMS). In Proceedings of the Ninth Biennial ASME Conference on *Engineering systems design and analysis ESDA08*, Haifa, Israel, 7-9 July 2008.

24 **Akcan, H., Kriakov, V., Brönnimann, H.,** and **Delis, A.** GPS free node localization in mobile wireless sensor networks. In Proceedings of *MobiDE'06*, Chicago, Illinois, USA, 2006.

25 **Hazas, M.** and **Ward, A.** A novel broadband ultrasonic location system. In Proceedings of the Fourth International Conference on *Ubiquitous computing (UbiComp 2002)*, Goteborg, Sweden, 2002, pp. 264–280.

26 **Parrilla, M., Anaya, J. J.,** and **Fritsch, C.** Digital signal processing techniques for high accuracy ultrasonic range measurements. *IEEE Trans. Instrumn Measmt*, August 1991, **40**(4), 759–764.

27 **Manthey, W.** and **Kroemer, N. V.** Ultrasonic transducers and transducer arrays for applications in air. *Measmt Sci. Technol.*, 1991, **3**(3), 249–261.

28 **Johansson, J., Gustafsson, M.,** and **Delsing, J.** Ultra-low power transmit/receive ASIC for battery operated ultrasound measurement systems. *Sensors and Actuators*, 2006, **125**, 317–328.

29 **Montgomery, D. C.** *Design and analysis of experiments – 7th edition*, 2008 (Wiley, New York).

30 **Box, G.E.P.** and **Cox, D.R.** An analysis of transformations. *J. Royal Stat. Soc. Series B*, 1964, **vol. 26**, pp. 1–78.

31 **Box, G. E. P., Hunter, W. G.,** and **Hunter, J. S.** *Statistics for experimenters*, 1978 (Wiley, New York).

32 **Magori, V.** Ultrasonic sensors in air. In Proceedings of Ultrasonics Symposium, IEEE, Cannes, France 1–4 November 1994, vol. 1, pp. 471–481.

33 **Godfrey, L. G., Orme, C. D.,** and **Santos Silva, J. M. C.** Simulation-based tests for heteroskedasticity in linear regression models: some further results. *Econometrics J.*, 2006, **9**, 76–97.

34 **Zhang, D., Rolt, S.,** and **Maropoulos, P. G.** Modelling and optimization of novel laser multilateration schemes for high-precision applications. *Measmt Sci. Technol*, 2005, **16**, 2541–2547.

35 **Jakevicius, L.** and **Demcenko, A.** Ultrasound attenuation dependence on air temperature in closed chambers. *Ultragarsas (Ultrasound)*, 2008, **63**(1), 18–22.

36 **Kino, G. S.** *Acoustic waves: devices, imaging, and analog signal processing*, 1987, Prentice-Hall, New Jersey.

37 **Kiménez, A. R.** and **Seco, F.** Precise localisation of archaeological findings with a new ultrasonic 3D positioning sensor. *Sensors and Actuators A*, 2005, **123–124**, 224–233.

38 **Ronchetti, E.** and **Staudte, R. G.** A robust version of Mallow's Cp. *J. Am. Statist. Ass.*, 1994, **89**, 550–559.

39 **Cross, N. R., Dotson, J. R., Flank, D. R., Peggs, G. N., Cox, M. G., Forbes, A. B., Corta, R., O'Donnell, J.,** and **Prieto, E.** A large reference artefact for CMM verification. National Physical Laboratory, NPL Report CLM 6, May 1998, 45 pp.

40 GUM. Guide to the expression of uncertainty in measurement. International Organization for Standardization, Geneva, Switzerland, 2004.

41 VIM. International vocabulary of basic and general terms in metrology. International Organization for Standardization, Geneva, Switzerland, 2004.

42 **Mastrogiacomo, L.** and **Maisano, D.** Network localization procedures for experimental evaluation of mobile spatial coordinate measuring system (MScMS). Submitted to *Int. J. Advd Mfg Technol.*, 2009.

43 **Toda, M.** Cylindrical PVDF film transmitters and receivers for air ultrasound. IEEE Transactions on *Ultrasonics, Ferroelectrics, and Frequency control*, 2002, **49**(5), 626–634.

44 **Toda, M.** and **Dahl, J.** PVDF corrugated transducer for ultrasonic ranging sensor. *Sensors and Actuators*, 2005, **134**, 427–435.

45 **Box, G. E. P.** and **Cox, D. R.** An analysis of transformations. *J. Royal Statist. Soc. Series B*, 1964, **26**, 1–78.

46 **Kino, G. S.** *Acoustic waves: devices, imaging, and analog signal processing*, 1987 (Prentice-Hall, New Jersey).